Shear Behavior of Flexible Polyurethane Foams Under Uniaxial Compression

Anna Andersson,[1] Stefan Lundmark,[1,2] Anders Magnusson,[2] Frans H. J. Maurer[1]

[1]*Department of Polymer & Materials Chemistry, Lund University, S-22100 Lund, Sweden*
[2]*Perstorp Specialty Chemicals AB, R&D, S-284 80 Perstorp, Sweden*

Received 19 June 2008; accepted 18 August 2008
DOI 10.1002/app.29244
Published online 18 November 2008 in Wiley InterScience (www.interscience.wiley.com).

ABSTRACT: The mechanisms behind the load building capabilities of a hyperbranched polymer (HBP) in polyurethane (PU) foams have been investigated, using microscopy techniques and mechanical analyses. By broadening the traditional uniaxial compression characterization of PU foams to include combined shear deformations and compression behavior, an apparent Poisson ratio of the foam could be obtained *in situ*. The Poisson ratio as function of uniaxial compression ratio of the foam was thus studied for foams filled with Styrene Acrylonitrile (SAN) and foams containing HBP. Generally a window of deformation ratios could be defined in which the Poisson ratio was negative. The width of this window varied systematically with the SAN loading, where an increase in SAN particle loading resulted in a broadening of the negative Poisson ratio window. © 2008 Wiley Periodicals, Inc. J Appl Polym Sci 111: 2290–2298, 2009

Key words: compression; microstructure; modulus; polyurethanes; shear

INTRODUCTION

Polyurethane foam

Polyurethane (PU) foam is the world's most frequently synthesized cellular solid with approximately 8 million tons produced annually.[1] Major applications of PU foams are insulation, furniture, packaging, and carpet cushioning. The research reported here aims to contribute to the knowledge of automotive seating materials, one of the largest application areas of flexible PU foams.

Flexible PU foam is produced in a step growth polymerization process. It can be performed either in a mold or in a semicontinuous slab stock process. The primary reactions are those involving the reaction between isocyanate groups and hydroxyl, amine or acid groups. Isocyanate reacts with alcohols to form urethane linkages, with amines to form urea groups, with organic acids to form amide linkages, and with water to form carbamic acid, which is subsequently converted to amines and carbon dioxide. The secondary reactions involve the reaction between isocyanate groups and the products from the primary reactions. Isocyanate reacts with urethane to form allophanate groups and with urea to form biuret groups.[2] The carbon dioxide formed in the primary reaction between water and isocyanate is responsible for the swelling of the polymer resulting in a foam. The foam consists of two phases, polymer making up the solid phase and air making up the gaseous phase. The carbon dioxide produced during the synthesis of the foam is rapidly replaced with air due to the open-cell nature of the foam.

The solid phase has a heterogeneous microstructure in itself. This heterogeneity consists of urea-rich precipitates, constituting the hard phase, and polyether urethanes, constituting the soft phase.[3,4] The structure can be further modified by the addition of styrene acrylonitrile (SAN) particles, Styrene-Acrylonitrile copolymers grafted on polyether polyol macromers, which act as hard polymeric fillers in the continuous solid phase of the PU foam. SAN particles are typically spherical with a diameter of about 0.05–1 μm, well dispersed in the polymer matrix[5,6] and added to increase firmness of the foam. The addition of multifunctional, hyperbranched polymer, HBP, also increases the firmness of PU foams. However, the mechanism behind its firmness increasing ability is not yet examined. Previous studies show that incorporation of a multifunctional, hyperbranched polymer (HBP) in PU foams together with low loadings of SAN, typically 5%, significantly enhances firmness.[7,8] No satisfactory explanation has been found to account for this behavior.

Flexible PU foams exhibit open-cell foam structures. The bicontinuous, heterogeneous material consists of a solid phase built-up by PU cell-struts and

Correspondence to: F. H. J. Maurer (frans.maurer@polymat.lth.se).
Contract grant sponsor: Perstorp Specialty Chemicals AB.

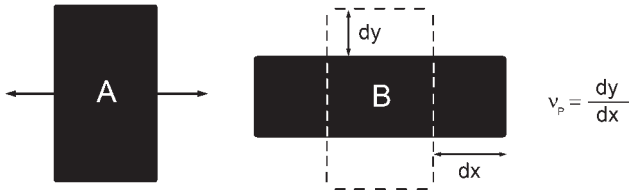

Figure 1 The Poisson ratio is defined as the negative ratio between the relative contraction normal to the load and the relative extension in the load direction. A is the original sample and B is the sample subjected, in this case, to a tensile force.

vertices and a gaseous phase consisting of air. The cell-struts meet at a vertex with an edge connectivity of four. Furthermore, the foam can be characterized by the number of struts making up a cell. This varies from three to seven struts for foams viewed in two dimensions. For further details in the three dimensional morphology, see 3D-microtomography work done by Elliott.[9]

Mechanical properties

Isotropic, elastic materials can be mechanically characterized by three basic elastic constants, according to the following equations:[10]

$$E = \frac{9KG}{3K + G} \tag{1}$$

where E is the uniaxial compression modulus, G is the shear modulus, and K is the bulk modulus. Furthermore:

$$\upsilon_P = \frac{3K - 2G}{2(3K + G)} \tag{2}$$

where ν_P is the Poisson ratio. In the isotropic case, only two of the constants in eq. (1) are independent, and the third one is determined by the other two. The Poisson ratio can therefore be calculated from E and G according to:

$$\upsilon_P = \frac{E}{2G} - 1 \tag{3}$$

The traditional way of evaluating the performance and making specifications of foams for automotive seating is by measuring the firmness by indentation force deflection (IFD), resilience by ball rebound, compression set, and uniaxial compression modulus. The uniaxial compression modulus—also known as support factor, measured as the ratio between 65% IFD and 25% IFD—has long been believed to be one of the most important specifications of a foam, because it governs comfort and durability. It is also directly coupled to the total vertical movement (TVM), which is an important specification of furniture design.[11] The traditional foam specifications are all connected to the compression behavior of the foam. It is unusual in the PU foam industry to look into the shear behavior of the foams, even though we believe these properties are equally relevant to the comfort in automotive seating. Surprisingly, this combined behavior in compression and shear has not received any attention in literature and therefore our study focus on the shear behavior and relationship between shear and compression behavior of flexible PU foams.

The Poisson ratio

The Poisson ratio is defined as the negative ratio of the relative contraction normal to the load to the relative extension in the direction of the load,[12] Figure 1. Almost all common materials exhibit positive Poisson ratios between 0.2 and 0.5. Foams in particular are shown to exhibit Poisson ratios of values close to 1/3,[12] independent of relative density and the amount of closed cells.

Materials having negative Poisson ratios, referred to as auxetic materials, contract when a compressive force is applied and expand under tension. This behavior contradicts what one intuitively expects from a material when subjected to a deformation. Two reviews cover the naturally occurring, synthesized and predicted Auxetic materials.[13,14] There are a few examples of naturally occurring auxetic materials. On the molecular level, negative Poisson ratios have been found in iron pyrites, in single crystal materials, such as arsenic and cadmium, and in many of the cubic elemental metals.[14] Moreover, there are examples of negative Poisson ratios found in biomaterials such as cow teat skin, cat skin, and load-bearing cancellous bone.[14] The first one to report creating a foam with negative Poisson ratio was Roderic Lakes in 1987.[15] He manipulated the Poisson ratio by compressing a polyester foam, heat treating it, and subsequently cooling it, to obtain foam which exhibited a negative Poisson ratio. Several others have produced and examined auxetic PU foams in a similar manner.[16–25] Each material reported has been altered to obtain cells with so called re-entrant[15] or inverted structures, see Figure 2. The Poisson ratios in these studies have been obtained by various image data detection methods.

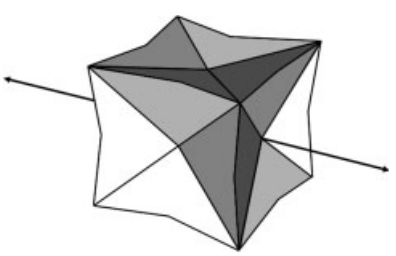

Figure 2 Re-entrant or inverted structure of a negative Poisson ratio material.

TABLE I
PU Foam Formulations

	P1	P2	P3	P4	N9	N13	B1
Polyol	87.6	62.7	37.8	13.0	84.9	79.5	91.1
Copolymer polyol – SAN	12.4	37.3	62.2	87.0	12.4	12.4	–
Hyperbranched polymer – Boltorn® H311	–	–	–	–	2.97	8.91	8.81
Toluene diisocyanate	49.9	49.3	48.7	48.0	54.9	57.9	51.6
Water	4.15	4.13	4.11	4.09	3.85	3.24	3.25
Surfactant – Y10184	0.7	0.7	0.7	0.7	0.7	0.7	0.7
Surfactant – DC 5169	0.3	0.3	0.3	0.3	0.3	0.3	0.3
DEOA-LF	1	1	1	1	1	1	1
NIAX A1	0.08	0.08	0.08	0.08	0.08	0.08	0.08
Dabco 33-LV	0.36	0.36	0.36	0.36	0.36	0.36	0.36
Glycerin	0.4	0.4	0.4	0.4	0.4	0.4	0.4

All components are given as parts per hundred polyol, pphp. pphp refers to weight of component in relation to hundred polyol, where polyol is the sum of polyol, copolymer polyol, and hyperbranched polymer.

Poisson ratio measurements have also been performed on conventional flexible PU foams;[26] however, the methodologies of obtaining the Poisson ratios in the literature differ from the novel methodology which will be demonstrated in this study. The purpose of the present study was to investigate the shear behavior of PU foams under uniaxial compression. During the course of the measurements it was found that the shear modulus exceeded the compression modulus for certain degrees of deformation. The moduli were employed to obtain an apparent Poisson ratio, which was used to describe the material when subjected to large uniaxial deformation.

MATERIALS AND MEASUREMENT TECHNIQUES

Materials

The polyol used was Hyperlite 1650, which is a reactive polyether polyol with OH-number 36 mg KOH/g and a theoretical functionality of 3. The copolymer polyol was Hyperlite 1656 with a solid content of 43% SAN particles in a base polyol with OH-number 31.5 mg KOH/g and a theoretical functionality 2.8. Boltorn® H311 was used as the hyperbranched polymer. The HBP is based on 2,2-dimethylolpropionic acid (bisMPA) with a molecular weight of 5000 g/mol and a OH number of 260 mg KOH/g. The toluene diisocyanate (TDI) was a 80/20 blend of 2,4- and 2,6-TDI. Water was taken directly from the tap. The foam formulations, including catalysts and surfactants, are reported in Table I.

Foam preparation

The foams were prepared at Perstorp Specialty Chemicals AB. Foams of different amounts of copolymer polyol and HBP according to Table II were synthesized batch wise in a closed mold with the dimensions 41 × 41 × 10 cm^3. All components except for the isocyanate were firstly stirred thoroughly in a plastic container. The isocyanate was subsequently added and the mixture stirred for an additional 4–5 s after which the formulation was directly added into the mold, at 58°C. The foam bun was removed from the mold after ca. 5 min and crushed to prevent foam collapse. The foam buns were sawed into planar sheets with a thickness of 25 mm. From these sheets, cylindrical samples were punched with a diameter of 25 mm. The thickness of the cylinders was oriented perpendicular to the rise direction of the foam.

Rheology

The shear compliance and uniaxial compression modulus were measured with a stress-controlled rheometer (AR2000, TA Instrument). The geometry used was 25-mm aluminum parallel plate. The cylindrical samples had a diameter of 25 mm and a thickness of approximately 25 mm. The sample was kept in position using double sided duct tape. The shear compliance was obtained at different levels of uniaxial compression (2, 5, 10, 20, 30, 40, and 60%) from a shear creep experiment of 1800 s, with a shear stress of 20 Pa performed at 25°C. The compliance was

TABLE II
Percentage Solids of SAN Particles and Hyperbranched Polymer in the Formulations

	P1	P2	P3	P4	N9	N13	B1
% Solid SAN	5	15	25	35	5	5	–
% Solid Boltorn® H311	–	–	–	–	2.5	7.5	7.5

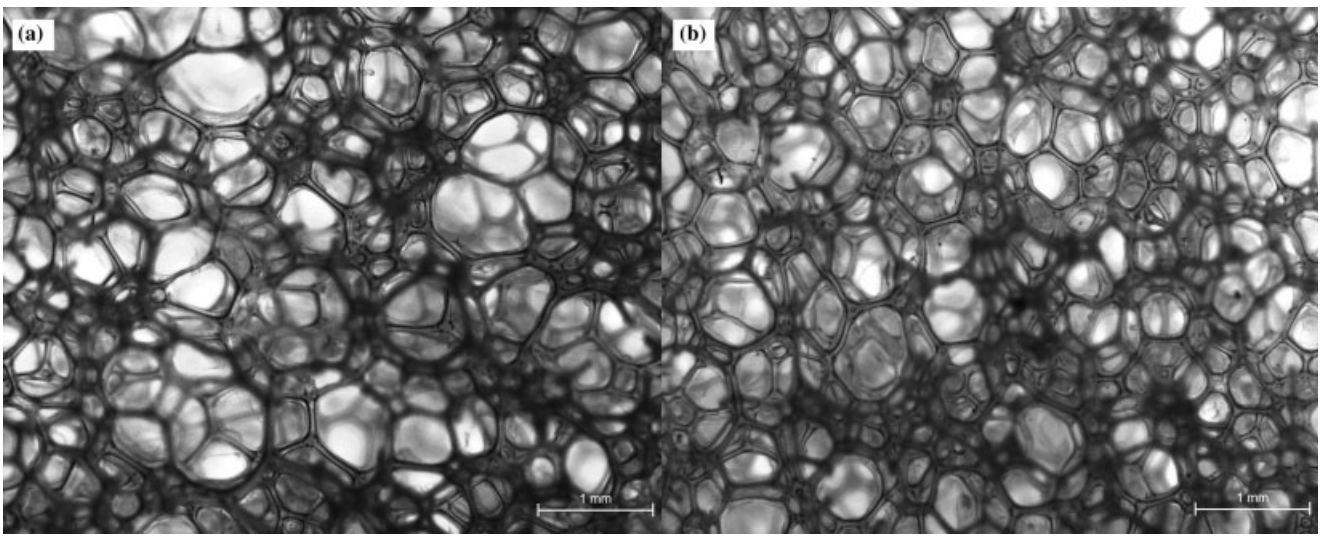

Figure 3 Stereo micrographs of polyurethane foam P1 (a) and N13 (b), containing SAN particles only and SAN particles plus hyperbranched polymers, respectively.

subsequently converted to shear modulus using the following elastic approximation:

$$G(t) = \frac{1}{J(t)} \tag{4}$$

where $G(t)$ is the shear modulus, $J(t)$ the shear compliance, and t is 1800 s. The uniaxial compression modulus, $E(\dot{\gamma})$ was obtained from a squeeze experiment, at 25°C, performed at 0.0556%/s, from the undeformed state until 60% uniaxial deformation. These two quantities were comparable due to corresponding and equivalent time scales. The apparent Poisson ratios were obtained by using eq. (3) and the calculated moduli. Strain sweeps of 0.01–10% strain and 1 Hz at different compression ratios were performed at 25°C for a sample containing 5% SAN and 2.5% HBP. Frequency sweeps between 100 and 0.1 Hz of a cubic sample with the side 25 mm, containing 5% SAN and 2.5% HBP were performed at 0.1% strain at 25°C. The measurement was performed in all three directions of the sample.

Dynamic mechanical analysis

Dynamic mechanical analysis (DMA) was carried out on a stress-controlled TA Instrument DMA 2980, in the compression mode. The samples were cylindrical with dimensions of 25 mm in diameter and approximately 5 mm thick. The samples were heated at 2°C/min from room temperature to 130°C with a frequency of 1 Hz and an amplitude of 50 μm.

Imaging

Optical microscopy on an Olympus stereo microscope was performed. The images were obtained using a Nikon, Infinity2 digital camera connected to the Infinity image processing software. To obtain images at different compression ratios of the foam, a sample holder with adjustable width was used.

Transmission electron microscope

A small piece (approximate 5 mm side length) of foam was cut and placed in a Petri dish and left for 3 days in the fumes from 2% OsO_4 solution. A tip of the stained foam was then placed in a beam capsule that was filled up with a hard epoxy embedding resin (TAAB812). The capsule was then placed in an oven at 60°C for 18 h for curing. A small square (approximate size 0.1 × 0.1 mm^2) was trimmed so that the stained foam strut was visible through the surface. Thin sections, less than 100 nm, were cut in a Leica Ultracut T ultramicrotome. The sections were picked up on a 600 Hex Cu grid. The sections were examined in a Philips 10 TEM (transmission electron microscope).

RESULTS AND DISCUSSION

Cell scale morphology

The flexible PU foams of this study were found to have densities between 30.7 and 33.8 kg/m^3, which were in the range of the estimations from the formulations. The cell morphology of foam containing 5% SAN particles and the foam containing 5% SAN particles as well as 7.5% hyperbranched polymers, can be viewed in Figure 3(a) and (b), respectively. Measurements of cell and strut dimensions resulted in the values of Table III. There are no fundamental differences in morphology in terms of degree of opened cells and dimension of cells between the different

TABLE III
Cell Dimensions of the PU Foams

Sample	Average cell diameter (μm)	Average strut thickness (μm)	Average PPI (pores per inch)
P1	303 ± 88	39 ± 11	62 ± 6
P4	243 ± 126	41 ± 5	68 ± 10
N13	287 ± 92	45 ± 10	60 ± 7

foam samples, see Table III. The incorporation of HBP does not have an influence on cell size or degree of open cells. Therefore, the explanation behind how SAN-filled foams versus SAN and HBP-filled foams behave differently probably does not lie in the cell scale morphology of the foams.

Mechanical properties

The stress-strain curves, in compression, for the flexible foams of this study are shown in Figure 4. The shape of the curves can be explained by the bending and buckling of cell struts. The initial linear region corresponds to the elastic bending of struts parallel to the compression direction. The plateau region at about 10–50% compression has been described as an effect of buckling of struts parallel to the compression direction.[12] However Elliott et al. have reported, by the help of 3D microtomography, that bending of struts inclined to the compression direction are responsible for the plateau region as well.[9] Careful examination by altering the focus of the foam images confirm that bending of cells that are oriented slightly off the direction parallel to the compression direction do occur in the plateau region. Following the plateau is a region of densification, which starts at about 55–60% deformation with a sharp increase of stress as a function of compression ratio. In this region, the cell struts have approached each other to the degree of making physical contact with each other, hence the sharp increase in stress at these deformations. The trends of the stress-strain curve are similar for all the foams examined in this study. The absolute values of the plateau stresses and moduli vary according to SAN loading and HBP content but the general appearances of the curves are the same. The one curve with a somewhat different behavior is foam sample N13, with the high content of HBP, where the transition from the linear region to the plateau region is sharper compared with the other samples.

DMA analyses were performed on each sample and the results are consistent with the stress-strain results, see Figure 5. The uniaxial compression modulus increases as function of both SAN content and HBP. It is worth noting that the slope of the HBP is steeper than the slope of SAN, indicating that the HBP is an efficient firmness enhancer in flexible PU foams, as described by Magnusson et al.[7,8] A temperature ramp in the interval from room temperature to 130°C for sample P3 generated the results of Figure 6. The drop in storage modulus corresponds to the T_g of SAN. This agrees well with the DSC results, which confirm a glass transition at 113°C. In Figure 7, the area under the tan delta is plotted as function of filler content, i.e., SAN and HBP. One can clearly see how the area increases as function of SAN loading and remain constant as function of HBP content as expected.

The mechanical behavior of a single cell exposed to compression for a foam containing 5% SAN and 7.5% HBP can be viewed in Figure 8. The foam sample has been compressed to 0, 5, 10, 20, 30, and 40%, and the same cell has been photographed

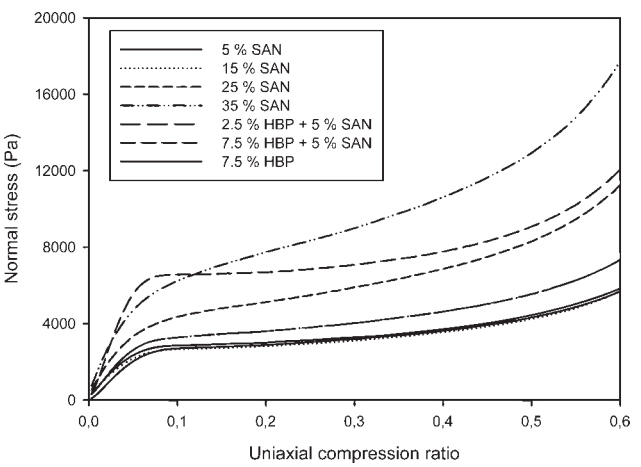

Figure 4 Stress as function of uniaxial compression ratio for P1 containing 5% SAN, P2 containing 15% SAN, P3 containing 25% SAN, P4 containing 35% SAN, N9 containing 5% SAN and 2.5% HBP, N13 containing 5% SAN and 7.5% HBP and B1 containing 7.5% HBP.

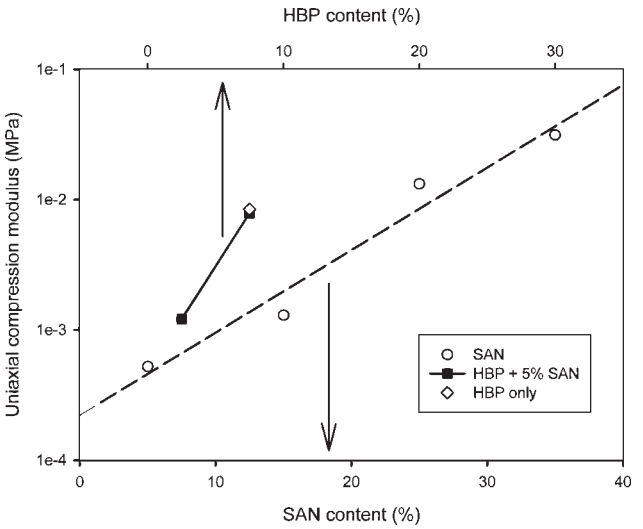

Figure 5 Uniaxial compression modulus as function of SAN content and HBP content as determined by DMA at 40°C.

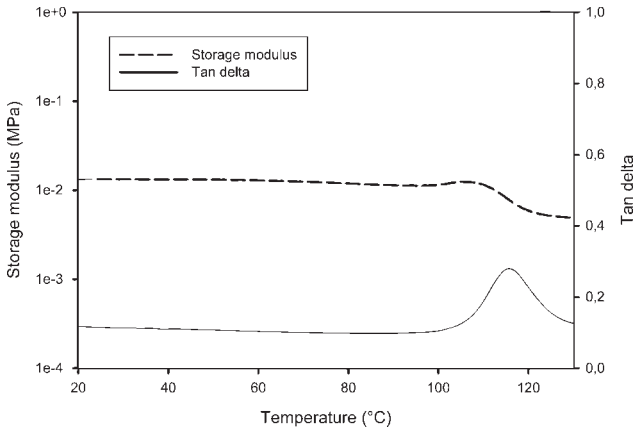

Figure 6 Results from the dynamic mechanical experiment performed on DMA for sample P3 containing 25% SAN.

throughout uniaxial compression. Bending of the cell struts occur from 5% compression and onwards. Buckling is evident from 20% compression. These behaviors were representative and consistent among all foam samples, as were the dimensions of the cells and cell struts. The results presented do not reveal any significant difference in how foams behave mechanically when they are reinforced with SAN filler particles or if they are loaded with hyperbranched polymer.

With the appearance of the stress-strain curve in Figure 8, the elastic modulus, E, must exhibit some interesting behavior as a function of compression ratio of the foam, considering eq. (5).

$$E = \frac{\partial \sigma}{\partial \varepsilon} \tag{5}$$

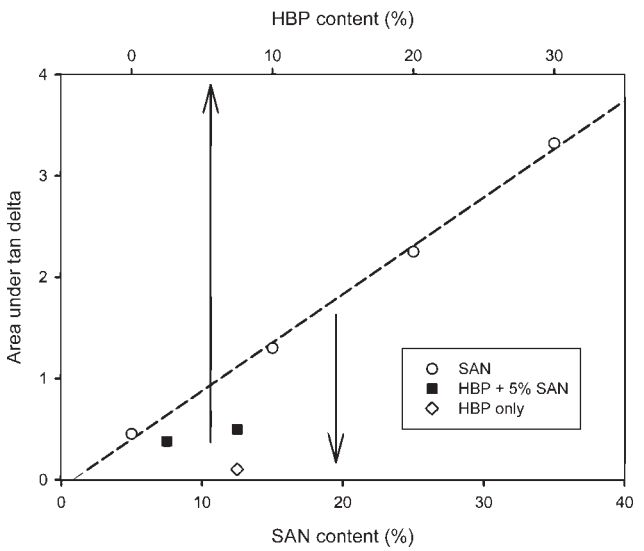

Figure 7 Area under tan delta as a function of SAN loading and HBP content.

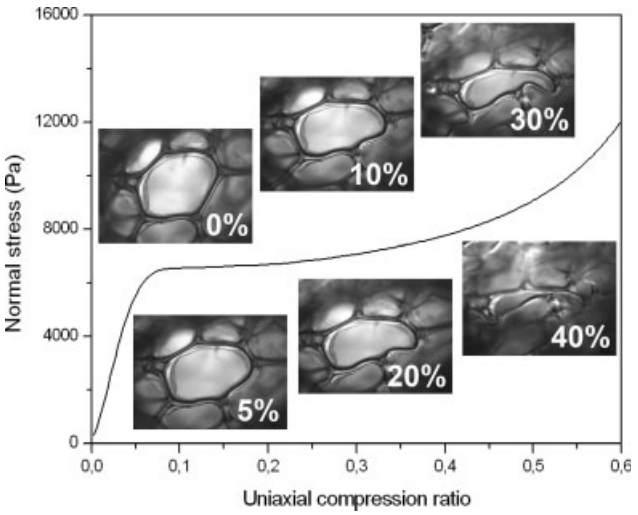

Figure 8 Stress-strain curve of a polyurethane foam showing microscopy images of the deformations 0, 5, 10, 20, 30, and 40%, at the single-cell scale.

The derivative of the E modulus with respect to the compression ratio generates the uniaxial compression modulus as a function of compression ratio, Figure 9. It is evident from the graph that the material decreases rapidly in modulus initially. It reaches a minimum value of the uniaxial compression modulus at about 10–12% compression, followed by an exponential increase up to 60% compression.

The corresponding shear modulus, G, was determined by a creep experiment at 20 Pa. The results are also shown in Figure 9. The shear modulus exhibits some similarities to the uniaxial compression modulus in that the stiffness decreases as a function of compression ratio initially and reaches a minimum value. However, the minimum appears at about 40% compression and not at 10% as for the uniaxial compression modulus. In a region between 10 and 40% compression, the shear modulus exhibit

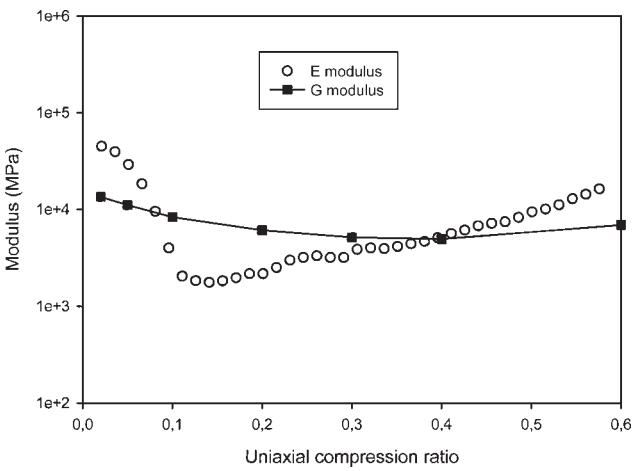

Figure 9 Uniaxial compression modulus, E, and shear modulus, G, of a polyurethane foam containing 5% SAN.

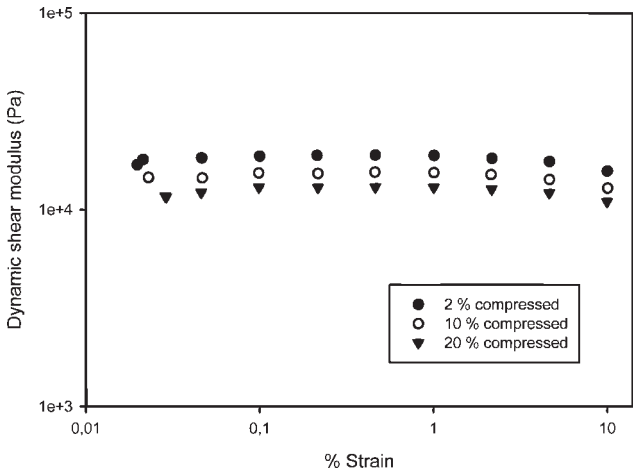

Figure 10 Strain sweeps performed at different compression ratios of a foam containing 5% SAN and 2.5% HBP.

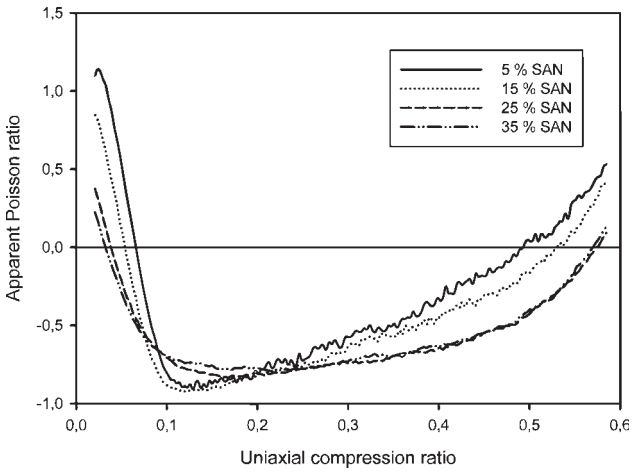

Figure 12 The Poisson ratio as a function of uniaxial compression ratio for PU foams containing 5, 15, 25, and 35% SAN.

a larger absolute value than the uniaxial compression modulus. This effect is caused by the shear modulus being less sensitive to deformation ratio, hence exhibits a slower decrease in modulus compared with the compression modulus. The materials examined are thus stiffer in the shear than in compression at these deformations.

The linearity of the stress distributions were examined by performing strain sweeps of one sample at different compressive deformations. The results are presented in Figure 10. As evident from the figure, the dynamic shear modulus is linear in a region between 0.1 and 2% strain and varies only as function of compression ratio, as also seen for the *G* modulus in Figure 9.

As the shear and uniaxial compression moduli are related to each other by the Poisson ratio, it is now possible to examine the change in Poisson ratio with compression, by using eq. (3). One should bear in mind that this equation is valid for isotropic, elastic materials at small deformations. Our materials are indeed isotropic in the undeformed state, confirmed by measuring shear moduli of one material in the three directions, see Figure 11. However, when the materials are deformed in one direction to as much as 60%, there is clearly anisotropy in the samples. The Poisson ratio obtained is therefore an apparent ratio. The results are presented in Figure 12 and Figure 13, for SAN and HBP containing foams, respectively. The appearance of the curves are similar for all foams, the apparent Poisson ratio starts at a high level at low deformations, decreasing as a function of compression ratio and reaches a minimum at about 10%. The surprisingly high values of the apparent Poisson ratios at low deformations could appear due to the fact that the foam samples were cut both at the top and bottom. Approximately 0.3 mm of the

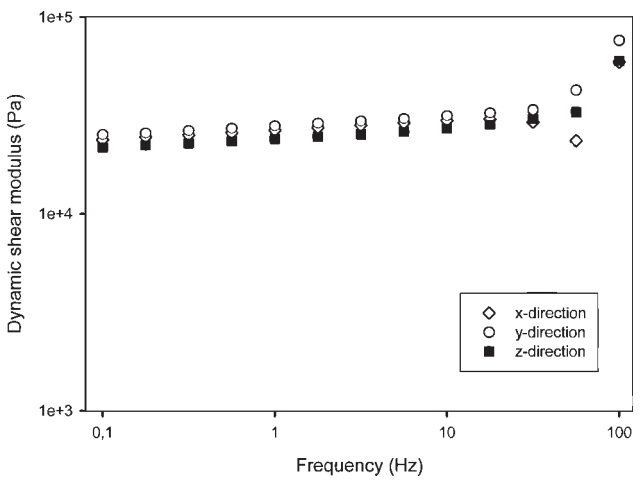

Figure 11 Dynamic shear modulus as function of frequency in the three directions of a foam containing 5% SAN and 2.5% HBP.

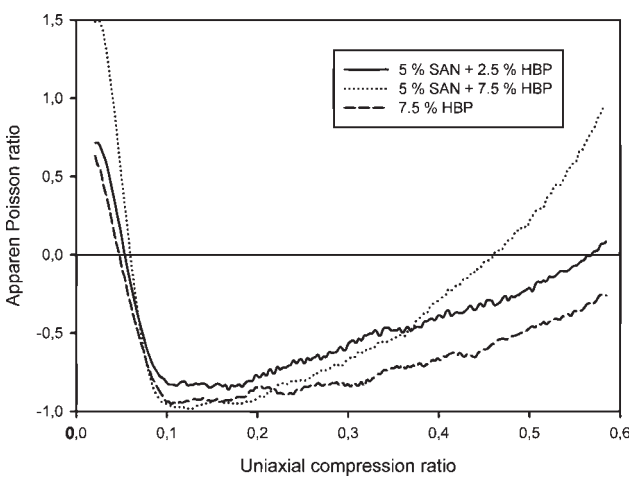

Figure 13 The Poisson ratio as a function of uniaxial compression ratio for PU foams containing 2.5 and 7.5% HBP.

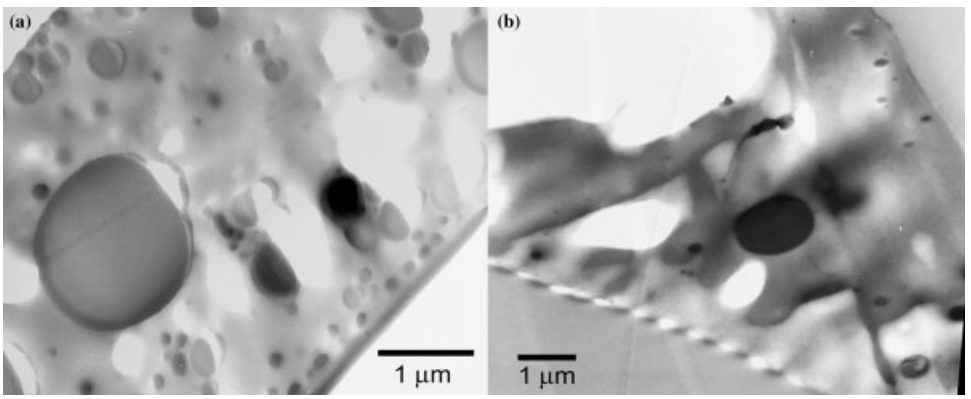

Figure 14 TEM images of (a) foam P4, containing 35% SAN and of (b) foam N13, containing 5% SAN and 7.5% HBP, showing the spherical SAN particles.

sample thickness (two times half the thickness of a layer of cells) are thus subjected to edge effects. When the sample has been compressed to overcome these edge effects, the Poisson ratio approaches the value of 0.3 which is the value most foams are found to have in their undeformed states. In the deformation range of 5–60%, negative values of apparent Poisson ratio are found, see Figures 12 and 13. It can be observed that an increased content of SAN particles result in a much broader range in which the foam exhibits negative values of the apparent Poisson ratio. The range in which the shear modulus is larger than the uniaxial compression modulus, that is, the deformation window in which the Poisson ratio is less than -0.5 follows a similar trend. Incorporation of the HBP does not result in such systematic variation of the deformation window.

Strut scale morphology

To further elucidate the mechanism behind the reinforcing capabilities of HBP filled PU foams, TEM was performed on two representative samples. The image of sample P4 containing 35% SAN [Fig. 14(a)] confirm that SAN particles of 0.1–2 μm are present in the sample. It is evident that the polymeric filler particles are dispersed in a continuous matrix, as previously described by Wilkes and coworkers.[5] The foam sample shown in Figure 14(b) (N13) contains both 5% SAN particles and 7.5% hyperbranched polymer. In this case, the SAN particles are still well dispersed and no clusters or any other trace of HBP can be seen. The large white areas of the TEM images are caused by degradation of the polymer from electron beam damages.

The reason for being able to replace large amounts of SAN particles with small amounts of HBP without interfering with the high firmness of the sample can be argued from a couple of different viewpoints. The HBP used has a high degree of functionality which makes it a highly potent crosslinker containing multiple hydroxyl groups available for reaction with isocyanate groups in the PU foam formation reactions. This could be one explanation for its contribution to high values of firmness. An alternative explanation is that the HBP molecules which have an approximate diameter of $\sim$ 3 nm,[27] i.e., significantly smaller than the SAN particles and rather in the same length scale as the hard segment urea domains, are dispersed and not reacted into the matrix and due to its high stiffness and density contribute to large firmness by acting as a filler. A third theory suggests aggregation of HBP molecules into clusters that are dispersed or partially reacted into the PU matrix. The aggregates would have a reinforcing effect on the foam, similar to that of fillers.

The images suggest that the HBP is either molecularly dispersed, forming a nanoscopic heterogeneity, in the polymer matrix or reacted into the polymer backbone, creating no additional heterogeneity, since no clusters were observed at this resolution. A combination of these two situations could also explain the high reinforcing effect of HPB in flexible PU foam.

CONCLUSIONS

In an attempt to identify the mechanisms governing the firmness enhancements of flexible PU foams filled with hyperbranched polymers it was shown that the HBP do not form aggregates in the PU matrix. A more probable scenario is that the HBP molecules are either reacted into the polymer backbone as an efficient crosslinker or molecularly dispersed in the polymer matrix. In the process of evaluating mechanical measurements, we found that by combining shear and compressive measurements, the apparent Poisson ratio of flexible PU can be studied as function of compression ratio. We could define a deformation window in which the foam exhibits auxetic behavior, i.e., their apparent Poisson ratios have negative values. An increased amount of SAN

particles in flexible polyurehtane foams lead to a broadening of this window, whereas the influence of HBP is more difficult to interpret.

Helen Hassander at the Department of Polymer and Materials, Lund University, is gratefully acknowledged for preparing the TEM images.

References

1. Ionescu, M. Chemistry and Technology of Polyols for Polyurethanes; Rapra Technology Ltd: Shawbury, 2005.
2. Woods, G. Flexible Polyurethane Foams; Applied Science Publishers: London, 1982.
3. Armistead, J. P.; Wilkes, G. L.; Turner, R. B. J Appl Polym Sci 1988, 35, 601.
4. Neff, R.; Adedeji, A.; Macosco, C. W.; Ryan, A. J. J Polym Sci Part B: Polym Phys 1998, 36, 573.
5. Kaushiva, B. D.; Dounis, D. V.; Wilkes, G. L. J Appl Polym Sci 2000, 78, 766.
6. Herrington, R.; Hock, K. Flexible Polyurethane Foams 2nd ed.; Dow Chemical Co.: Midland, 1998.
7. Magnusson, A. MSc Thesis; Dendritic Polymer Polyol as Load Builder in High Resilience Polyurethane Foam; University of Surrey, Surrey, 2006.
8. Magnusson, A.; Midelf, B.; Häggman, B. Dendritic Polymer Polyol as Load Builder in HR PU Foam; Polyurethanes EXPO, Orlando, FL, 2003.
9. Elliott, J. A. J Mat Sci 2002, 37, 1547.
10. Schwarzl, F. R. Polymer Mechanik; Springer Verlag: Berlin, 1990.
11. Polyurethane Foam Association Inc., In Touch Technical Bulletin, 1993, 3, 1.
12. Gibson, L. J.; Ashby, M. F. Cellular Solids 2nd ed.; Cambridge University Press: Cambridge, 1997.
13. Yang, W.; Li, Z.; Xie, B.; Yang, M. J Mater Sci 2004, 39, 2369.
14. Evans, K. E.; Alderson, A. Adv Mater 2000, 12, 617.
15. Lakes, R. S. Science 1987, 235, 1038.
16. Choi, J. B.; Lakes, R. S. Int J Mech Sci 1995, 37, 51.
17. Chan, N.; Evans, K. E. J Mater Sci 1997, 32, 5945.
18. Chan, N.; Evans, K. E. J Cell Plast 1999, 35, 130.
19. Chan, N.; Evans, K. E. J Cell Plast 1999, 35, 166.
20. Smith, C. W.; Grima, J. N.; Evans, K. E. Acta Mater 2000, 48, 4349.
21. Scarpa, F.; Cliffo, L. G.; Yates, J. R. Smart Mater Struct 2004, 13, 49.
22. Scarpa, F.; Pastorino, P.; Garelli, A.; Patsias, S.; Ruzzene, M. Phys Stat Sol 2005, 242, 681.
23. Gaspar, N.; Smith, C. W.; Miller E. A.; Seidler, G. T.; Evans, K. E. Phys Stat Sol 2005, 242, 550.
24. Bezazi, A.; Scarpa, F. Int J Fatigue 2007, 29, 922.
25. Pastorino, P.; Scarpa, F.; Patsias, S.; Yates, R. J.; Haake, S. J.; Ruzzene, M. Phys Stat Sol 2007, 244, 955.
26. Widdle, R. D.; Bajaj, A. K.; Davies, P. Int J Eng Sci 2008, 46, 31.
27. Rogunova, M.; Lynch, T. Y. S.; Pretzer, W.; Kulzick, M.; Hiltner, A.; Baer, E. J Appl Polym Sci 2000, 77, 1207.